

See discussions, stats, and author profiles for this publication at: <https://www.researchgate.net/publication/12033139>

# Novel Dinuclear Luminescent Compounds Based on Iridium(III) Cyclometalated Chromophores and Containing Bridging Ligands with Ester-Linked Chelating Sites §

ARTICLE *in* INORGANIC CHEMISTRY · APRIL 2001

Impact Factor: 4.76 · DOI: 10.1021/ic000212x · Source: PubMed

CITATIONS

61

READS

15

5 AUTHORS, INCLUDING:



Francesco Neve

Università della Calabria

82 PUBLICATIONS 1,948 CITATIONS

SEE PROFILE



Alessandra Crispini

Università della Calabria

127 PUBLICATIONS 2,662 CITATIONS

SEE PROFILE



Frédérique Loiseau

University Joseph Fourier - Grenoble 1

11 PUBLICATIONS 129 CITATIONS

SEE PROFILE



Sebastiano Campagna

Università degli Studi di Messina

246 PUBLICATIONS 12,413 CITATIONS

SEE PROFILE

# Novel Dinuclear Luminescent Compounds Based on Iridium(III) Cyclometalated Chromophores and Containing Bridging Ligands with Ester-Linked Chelating Sites<sup>§</sup>

Francesco Neve,<sup>\*,†</sup> Alessandra Crispini,<sup>‡</sup> Scolastica Serroni,<sup>‡</sup> Frédérique Loiseau,<sup>‡</sup> and Sebastiano Campagna<sup>\*,‡</sup>

Dipartimento di Chimica, Università della Calabria, I-87030 Arcavacata di Rende (CS), Italy, and Dipartimento di Chimica Inorganica, Chimica Analitica e Chimica Fisica, Università di Messina, via Sperone 31, I-98166 Messina, Italy

Received February 25, 2000

The syntheses and study of the spectroscopic, redox, and photophysical properties of a new set of species based on Ir(III) cyclometalated building blocks are reported. This set includes three dinuclear complexes, that is, the symmetric (with respect to the bridging ligand) diiridium species  $[(ppy)_2Ir(\mu-L-OC(O)-C(O)O-L)Ir(ppy)_2][PF_6]_2$  (**5**;  $ppy$  = 2-phenylpyridine anion;  $L-OC(O)-C(O)O-L$  = bis[4-(6'-phenyl-2,2'-bipyridine-4'-yl)phenyl]-benzene-1,4-dicarboxylate), the asymmetric diiridium species  $[(ppy)_2Ir(\mu-L-OC(O)-L)Ir(ppy)_2][PF_6]_2$  (**3**;  $L-OC(O)-L$  = 4-[(6'-phenyl-2,2'-bipyridine-4'-yl)benzoyloxy]phenyl}-6'-phenyl-2,2'-bipyridine), and the mixed-metal Ir–Re species  $[(ppy)_2Ir(\mu-L-OC(O)-L)Re(CO)_3Br][PF_6]$  (**4**). Syntheses, characterization, and spectroscopic, photophysical, and redox properties of the model mononuclear compounds  $[Ir(ppy)_2(L-OC(O)-L)][PF_6]$  (**2**) and  $[Re(CO)_3(L-COOH)Br]$  (**6**;  $L-COOH$  = 4'-(4-carboxyphenyl)-6'-phenyl-2,2'-bipyridine) are also reported, together with the syntheses of the new bridging ligands  $L-OC(O)-L$  and  $L-OC(O)-C(O)O-L$ . The absorption spectra of all the complexes are dominated by intense spin-allowed ligand-centered (LC) bands and by moderately intense spin-allowed metal-to-ligand charge-transfer (MLCT) bands. Spin-forbidden MLCT absorption bands are also visible as low-energy tails at around 470 nm for all the complexes. All the new species exhibit metal-based irreversible oxidation and bipyridine-based reversible reduction processes in the potential window investigated (between +1.80 and –1.70 V vs SCE). The redox behavior indicates that the metal-based orbitals are only weakly interacting in dinuclear systems, whereas the two chelating halves of the bridging ligands exhibit noticeable electronic interactions. All the complexes are luminescent both at 77 K and at room temperature, with emission originating from triplet MLCT states. The luminescence properties are temperature- and solvent-dependent, in accord with general theories: emission lifetimes and quantum yields increase on passing from acetonitrile to dichloromethane fluid solution and from room-temperature fluid solution to 77 K rigid matrix. In the dinuclear mixed-chromophore species **3** and **4**, photoinduced energy transfer across the ester-linked bridging ligands seems to occur with low efficiency.

## Introduction

The design of luminescent and redox-active multinuclear polypyridine metal complexes continues to attract great interest in light of the key role that these species currently play in the development of multicomponent assemblies featuring photoinduced made-to-order properties.<sup>1–6</sup> In particular, multinuclear polypyridine metal complexes contribute extensively to the development of artificial antennas for the photochemical conversion of solar energy<sup>7–10</sup> and as active elements for the elaboration and storage of information at the molecular level.<sup>11–15</sup>

Most of the systems investigated so far are based on Ru(II) building blocks, with Os(II) and Re(I) species also playing leading roles.<sup>2</sup> However, Ir(III) cyclometalated complexes have recently been the object of increasing interest because the excited-state properties of these species can be competitive with respect to those of ruthenium systems<sup>16–20</sup> (for example,

<sup>§</sup> Dedicated to Professor Alan L. Balch on the occasion of his 60th birthday.

<sup>\*</sup> To whom correspondence should be addressed. E-mail: f.neve@unical.it or photochem@chem.unime.it.

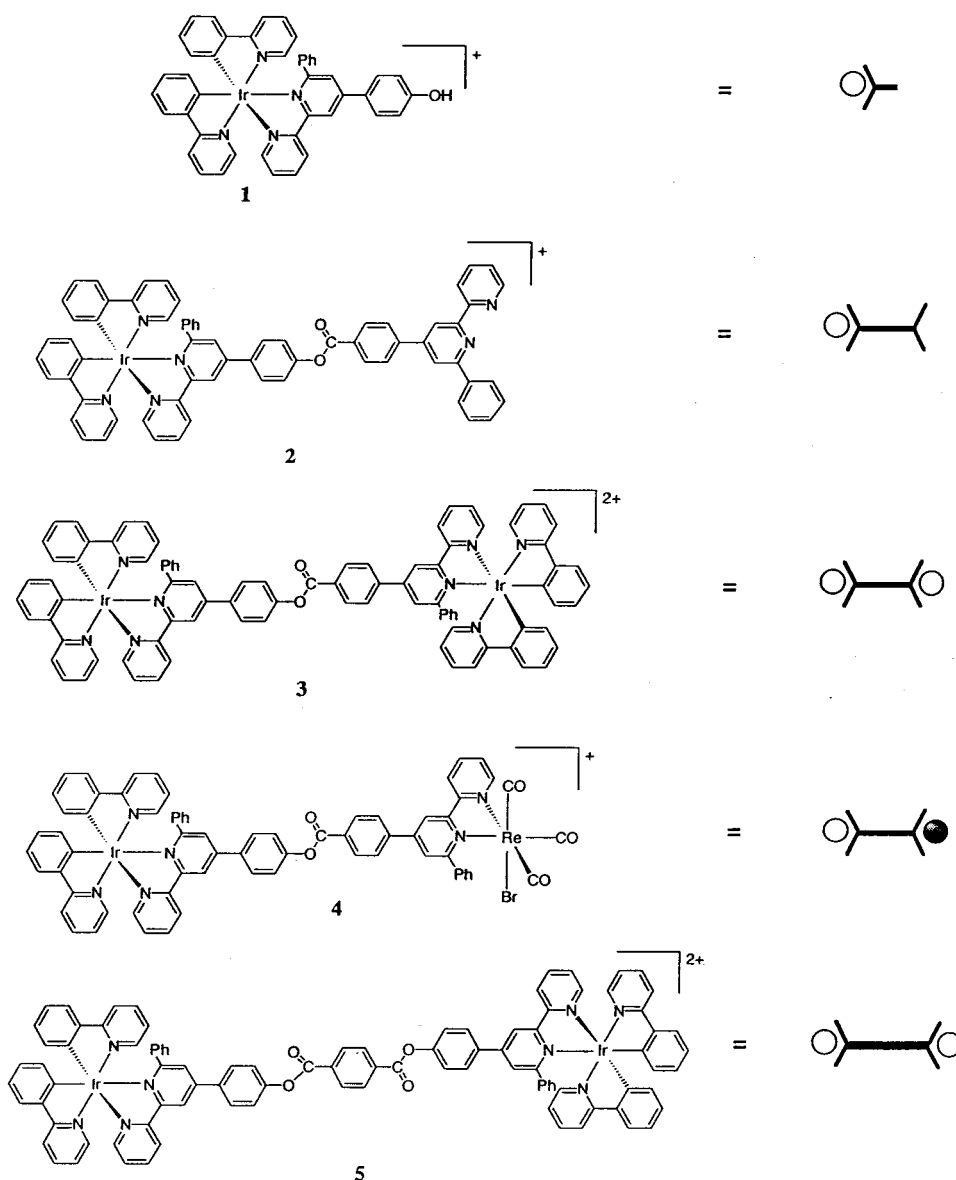
<sup>†</sup> Università della Calabria.

<sup>‡</sup> Università di Messina.

- (1) Sauvage, J.-P.; Collin, J.-P.; Chambron, J.-C.; Guillerez, S.; Coudret, C.; Balzani, V.; Barigelli, F.; De Cola, L.; Flamigni, L. *Chem. Rev.* **1994**, *94*, 993.
- (2) Balzani, V.; Juris, A.; Venturi, M.; Campagna, S.; Serroni, S. *Chem. Rev.* **1996**, *96*, 759.
- (3) Harriman, A.; Ziessel, R. *Chem. Commun.* **1996**, 1707.
- (4) Shaw, J. R.; Sadler, G. S.; Wacholtz, W. F.; Ryu, C. K.; Schmehl, R. H. *New J. Chem.* **1996**, *20*, 749.
- (5) De Cola, L.; Belser, P. *Coord. Chem. Rev.* **1998**, *177*, 301.
- (6) Barigelli, F.; Flamigni, L. *Chem. Soc. Rev.* **2000**, *29*, 1.

- (7) Balzani, V.; Juris, A.; Venturi, M.; Campagna, S.; Serroni, S. *Acc. Chem. Res.* **1998**, *31*, 26.
- (8) Slate, C. A.; Striplin, D. R.; Moss, J. A.; Chen, P.; Erickson, B. W.; Meyer, T. J. *J. Am. Chem. Soc.* **1998**, *120*, 4885.
- (9) Hu, Y.-Z.; Tsukiji, S.; Shinkai, S.; Oishi, S.; Hamachi, I. *J. Am. Chem. Soc.* **2000**, *122*, 241.
- (10) Campagna, S.; Serroni, S.; Puntoriero, F.; Di Pietro, C. In *Electron Transfer in Chemistry*; Balzani, V., Ed.; VCH-Wiley: Vol. 5, in press.
- (11) Beer, P. D.; Szemes, F.; Balzani, V.; Salà, C. M.; Drew, M. G.; Dent, S. W.; Maestri, M. *J. Am. Chem. Soc.* **1997**, *119*, 11864.
- (12) Barigelli, F.; Flamigni, L.; Collin, J.-P.; Sauvage, J.-P. *Chem. Commun.* **1997**, 333.
- (13) Waldmann, O.; Hassmann, J.; Müller, P.; Hanan, G. S.; Volkmer, D.; Schubert, U. S.; Lehn, J.-M. *Phys. Rev. Lett.* **1997**, *78*, 3390.
- (14) Bassani, D. M.; Lehn, J.-M.; Fromm, K.; Fenske, D. *Angew. Chem., Int. Ed. Engl.* **1998**, *37*, 2364.
- (15) Zahavy, E.; Fox, M. A. *Chem. Eur. J.* **1998**, *4*, 1647.
- (16) Crosby, G. A. *Acc. Chem. Res.* **1975**, *8*, 231.
- (17) Ayala, N. P.; Flynn, C. M., Jr.; Sacksteder, L. A.; Demas, J. N.; De Graff, B. A. *J. Am. Chem. Soc.* **1990**, *112*, 3837.
- (18) van Diemen, J. H.; Hage, R.; Lempers, H. E. B.; Reedijk, J.; Vos, J. G.; De Cola, L.; Barigelli, F.; Balzani, V. *Inorg. Chem.* **1992**, *31*, 3518.

Chart 1



luminescence quantum yields of iridium cyclometalated species are often larger than those of analogous ruthenium compounds having the same excited-state energy and the former compounds are usually better photoreductants than the latter) and new synthetic strategies have become available.<sup>21,22</sup>

We report here the syntheses and a thorough study of the spectroscopic, redox, and photophysical properties (both in butyronitrile rigid matrix at 77 K and in acetonitrile and dichloromethane fluid solutions at room temperature) of a new set of species based on Ir(III) cyclometalated building blocks, **2–5** (for the structural formulas of the new compounds, see Chart 1. The peripheral ligands of the Ir(III) subunits are 2-phenylpyridine anions). This set includes three dinuclear complexes, that is, the symmetric (with respect to the bridging ligand) diiridium species **5**, the asymmetric diiridium species

**3**, and the mixed-metal Ir–Re species **4**. Syntheses, characterization, and spectroscopic, photophysical, and redox properties of the model mononuclear compounds **2** and **6** are also reported. We point out that, to the best of our knowledge, **4** is the first luminescent mixed-metal Ir–Re species reported so far.

As bridging ligands for the dinuclear species, we used spacers containing ester linkages connecting phenylbipyridine sites. Ester linkages have not been exploited so far for the syntheses of multimetallic luminescent species, so this study is also useful for investigating whether these connections, potentially very versatile from a synthetic viewpoint, guarantee enough electronic communication between the photo- and redox-active subunits to allow efficient photoinduced energy-transfer processes.<sup>23</sup>

## Experimental Section

**General Procedures.** The <sup>1</sup>H NMR (300.13 MHz) spectra were recorded at room temperature with a Bruker AC 300 spectrometer;

- (19) Schmid, B.; Garces, F. O.; Watts, R. J. *Inorg. Chem.* **1994**, *33*, 9.  
 (20) Calogero, G.; Giuffrida, G.; Serroni, S.; Ricevuto, V.; Campagna, S. *Inorg. Chem.* **1995**, *34*, 541.  
 (21) Mamo, A.; Stefo, I.; Parisi, M. F.; Credi, A.; Venturi, M.; Di Pietro, C.; Campagna, S. *Inorg. Chem.* **1997**, *36*, 5947.  
 (22) Collin, J.-P.; Dixon, I. M.; Sauvage, J.-P.; Williams, J. A. G.; Barigelletti, F.; Flamigni, L. *J. Am. Chem. Soc.* **1999**, *121*, 5009.

- (23) It has been demonstrated that even electronic interactions as small as 10 cm<sup>-1</sup> are enough to allow fast energy and electron-transfer processes (see: Scandola, F.; Indelli, M. T.; Chiorboli, C.; Bignozzi, C. A. *Top. Curr. Chem.* **1990**, *158*, 73.).

chemical shifts are referenced to internal SiMe<sub>4</sub>. FT-IR spectra were recorded on a Perkin-Elmer 2000 spectrophotometer for KBr pellets. Elemental analyses were performed using a Perkin-Elmer 2400 microanalyzer. Electrochemical measurements were carried out in argon-purged acetonitrile at room temperature with a PAR 273 multipurpose equipment interfaced to a PC. The working electrode was a glassy carbon (8 mm<sup>2</sup>, Amel) electrode. The counter electrode was a Pt wire, and the reference electrode was an SCE separated with a fine glass frit. The concentrations of the complexes were about  $5 \times 10^{-4}$  M. Tetrabutylammonium hexafluorophosphate was used as supporting electrolyte, and its concentration was 0.05 M. Cyclic voltammograms were obtained at scan rates of 20, 50, 200, and 500 mV/s. For reversible processes, half-wave potentials (vs SCE) were calculated as the average of the cathodic and anodic peaks. The criteria for reversibility were the separation between cathodic and anodic peaks, the close-to-unity ratio of the intensities of the cathodic and anodic currents (ratios between 0.95 and 1.05 were considered acceptable), and the constancy of the peak potential on changing scan rate. The number of exchanged electrons was measured with differential pulse voltammetry (DPV) experiments performed with a scan rate of 20 mV/s, a pulse height of 75 mV, and a duration of 40 ms. Details of the method used for determining the number of the electrons, as well as the cyclic voltammograms and DPV curves for the complexes studied, are given in Supporting Information. For irreversible processes, the values reported are the peaks estimated by DPV. Absorption spectra were recorded with a Kontron Uvikon 860 spectrophotometer. Luminescence spectra were performed with a Spex-Jobin Yvon Fluoromax-2 spectrofluorimeter equipped with a Hamamatsu R3896 photomultiplier and were corrected for photomultiplier response using a program purchased with the fluorimeter. Emission lifetimes were measured with an Edinburgh FL-900 single-photon counting device (nitrogen discharge; pulse width, 3 ns). Emission quantum yields were measured at room temperature (20 °C) using the optically dilute method.<sup>24</sup> [Ru(bpy)<sub>3</sub>]<sup>2+</sup> (bpy = 2,2'-bipyridine) in aerated aqueous solution was used as a quantum yield standard, assuming a value of 0.028.<sup>25</sup> Experimental uncertainties were as follows: absorption maxima,  $\pm 2$  nm; molar absorption coefficient, 10%; emission maxima,  $\pm 4$  nm; luminescence lifetimes, 10%; luminescence quantum yields, 20%; redox potentials,  $\pm 10$  mV.

**Materials.** Re(CO)<sub>5</sub>Br and 1,4-bis(chlorocarbonyl)benzene were purchased from Aldrich and used as received. [Ir(ppy)<sub>2</sub>Cl]<sub>2</sub> was prepared as reported in the literature.<sup>26</sup> The syntheses of the ligands 4'-(4-hydroxyphenyl)-6'-phenyl-2,2'-bipyridine (L-OH)<sup>27</sup> and 4'-(4-carboxyphenyl)-6'-phenyl-2,2'-bipyridine (L-COOH),<sup>28</sup> as well as that of the complex [Ir(ppy)<sub>2</sub>(L-OH)][PF<sub>6</sub>]<sub>2</sub> (**1**),<sup>28</sup> have been reported previously. All other reagents and solvents (including dry solvents) were used as received from Aldrich. However, the supporting electrolytes and the glassware employed for the electrochemical experiments were stored in an oven for at least 24 h before use.

**Synthesis of the Ligands.** 4'-[(6'-Phenyl-2,2'-bipyridine-4'-yl)-benzoyloxy]phenyl-6'-phenyl-2,2'-bipyridine (L-OC(O)-L). The acid L-COOH (0.061 g, 0.173 mmol) was suspended in benzene (3 mL) and heated to reflux with an excess of thionyl chloride (1 mL) for 16 h. The solvent (and the excess of thionyl chloride) was removed under reduced pressure, and the crude acid chloride L-COCl was then used without further purification. The acid chloride and L-OH (0.055 g, 0.173 mmol) were added to degassed dichloromethane (50 mL) and stirred under a nitrogen atmosphere to give a white suspension. A colorless solution was formed just after the subsequent addition of triethylamine (5–6 drops). Stirring was continued for 5 h. After this time, the solvent was concentrated and washed with water (3  $\times$  25 mL). The organic phase was dried over Na<sub>2</sub>SO<sub>4</sub> and the solvent removed in vacuo. The resulting white residue was separated from minor

impurities by column chromatography over silica with CH<sub>2</sub>Cl<sub>2</sub>/3% MeOH as eluant (*R<sub>f</sub>* = 0.82). The product was recovered as a white solid (0.095 g, 84%). IR (KBr, cm<sup>-1</sup>):  $\nu(\text{COO})$  1740. <sup>1</sup>H NMR (CDCl<sub>3</sub>):  $\delta$  (ppm) 8.73–8.61 (m, 6 H), 8.41 (d, *J* = 8.5 Hz, 2 H, H<sup>a</sup>), 8.30–8.21 (m, 4 H'), 8.03 (s, 1 H), 8.00 (s, 1 H), 7.98 (d, *J* = 8.5 Hz, 2 H, H<sup>d</sup>), 7.93 (d, *J* = 8.5 Hz, 2 H, H<sup>a</sup>), 7.91–7.85 (m, 2 H), 7.59–7.47 (m, 6 H), 7.44 (d, *J* = 8.5 Hz, 2 H, H<sup>b</sup>), 7.39–7.34 (m, 2 H). Anal. Calcd for C<sub>45</sub>H<sub>30</sub>N<sub>4</sub>O<sub>2</sub>: C, 82.04; H, 4.59; N, 8.51. Found: C, 82.88; H, 4.71; N, 8.44.

**Bis[4-(6'-phenyl-2,2'-bipyridine-4'-yl)phenyl]-benzene-1,4-dicarboxylate (L-OC(O)-C(O)O-L).** A solution of L-OH (0.065 g, 0.2 mmol) in dry THF (16 mL) was treated under nitrogen with 1,4-bis(chlorocarbonyl)benzene (0.02 g, 0.1 mmol) and a few drops of triethylamine. The clear, pale-yellow solution turned into a suspension within 1–2 min. After it was stirred for 24 h, the solid was separated by filtration and the filtrate rotary-evaporated to dryness. The solid residue was redissolved in chloroform (30 mL), and the solution was consecutively washed with water (2  $\times$  25 mL), 0.1 M HCl (2  $\times$  25 mL), and water (2  $\times$  25 mL). The organic phase was dried over Na<sub>2</sub>SO<sub>4</sub> and the solvent removed in vacuo. The crude product was purified through chromatography over silica (CH<sub>2</sub>Cl<sub>2</sub>/10% MeOH). The pure product was obtained as a white solid (0.067 g, 86%). IR (KBr, cm<sup>-1</sup>):  $\nu(\text{COO})$  1738. <sup>1</sup>H NMR (CDCl<sub>3</sub>):  $\delta$  (ppm) 8.73 (br d, 1 H, H<sup>b</sup>), 8.71 (d, *J* = 8.8 Hz, 1 H, H<sup>3</sup>), 8.67 (br s, 1 H, H<sup>3'</sup>), 8.40 (s, 2 H, H<sup>c</sup>), 8.23 (d, *J* = 6.9 Hz, 2 H, H<sup>2',6'</sup>), 8.00 (s, 1 H, H<sup>5</sup>), 7.93 (d, *J* = 8.8 Hz, 2 H, H<sup>a</sup>), 7.89 (td, *J* = 7.9, 7.5, 2.0 Hz, 1 H, H<sup>4</sup>), 7.58–7.47 (m, 3 H, H<sup>3'',4'',5''</sup>), 7.43 (d, *J* = 8.8 Hz, 2 H, H<sup>b</sup>), 7.34 (m, 1 H, H<sup>5</sup>). Anal. Calcd for C<sub>52</sub>H<sub>34</sub>N<sub>4</sub>O<sub>4</sub>: C, 80.19; H, 4.40; N, 7.19. Found: C, 79.16; H, 4.36; N, 6.82.

**Synthesis of the Complexes.** [Ir(ppy)<sub>2</sub>(L-OC(O)-L)][PF<sub>6</sub>]<sub>2</sub> (**2**). The acid chloride L-COCl was freshly prepared as reported above for the synthesis of L-OC(O)-L. Solid [(ppy)<sub>2</sub>Ir(L-OH)][PF<sub>6</sub>]<sub>2</sub> (**1**) (0.069 g, 0.071 mmol) was added to a suspension of L-COCl (0.026 g, 0.071 mmol) in degassed dichloromethane (50 mL) under nitrogen. The resulting orange suspension turned clear upon addition of a few drops of triethylamine. The solution was stirred at room temperature for 48 h, then filtered. Evaporation of the solvent under reduced pressure gave a crude orange product (0.085 g), which was purified by chromatography over neutral alumina with a mixture of methanol (3%) in dichloromethane as eluant (*R<sub>f</sub>* = 0.89). Yield, 0.078 g (84%). IR (KBr, cm<sup>-1</sup>):  $\nu(\text{COO})$  1737,  $\nu(\text{PF})$  845. <sup>1</sup>H NMR (CD<sub>3</sub>CN):  $\delta$  (ppm) 8.84 (d, *J* = 1.8 Hz, 1 H, H<sup>3</sup>), 8.77–8.69 (m, 3 H), 8.74 (d, *J* = 1.5 Hz, 1 H, H<sup>3'</sup> of free L moiety), 8.39–8.32 (m, 4 H), 8.25 (d, *J* = 1.5 Hz, 1 H, H<sup>5'</sup> of free L moiety), 8.19–8.09 (m, 6 H), 8.01–7.80 (m, 7 H), 7.79 (d, *J* = 1.8 Hz, 1 H, H<sup>5</sup>), 7.66 (d, *J* = 5.1 Hz, 1 H), 7.62–7.53 (m, 5 H), 7.49–7.44 (m, 2 H), 7.31 (d, *J* = 7.8 Hz, 1 H), 7.18–7.09 (m, 2 H), 6.98–6.92 (m, 2 H), 6.83 (td, *J* = 7.4, 7.4, 1.4 Hz, 1 H), 6.77 (t, *J* = 7.7, 2 H), 6.65 (vbr s, 2 H), 6.58 (t, *J* = 7.7 Hz, 1 H), 6.38 (td, *J* = 7.4, 7.4, 1.4 Hz, 1 H), 5.97 (d, *J* = 7.3 Hz, 1 H), 5.59 (d, *J* = 7.4 Hz, 1 H). Anal. Calcd for C<sub>67</sub>H<sub>46</sub>F<sub>6</sub>IrN<sub>6</sub>O<sub>2</sub>: C, 61.69; H, 3.55; N, 6.44. Found: C, 62.12; H, 3.67; N, 6.32.

[Ir(ppy)<sub>2</sub>Ir(μ-L-OC(O)-L)Ir(ppy)<sub>2</sub>][PF<sub>6</sub>]<sub>2</sub> (**3**). [Ir(ppy)<sub>2</sub>Cl]<sub>2</sub> (0.011 g, 0.0103 mmol) and complex **2** (0.027 g, 0.0206 mmol) were suspended in a CH<sub>2</sub>Cl<sub>2</sub>/MeOH (4 mL/6 mL) mixture. Reflux of the stirred reaction mixture for 3 h afforded an orange solution. After it was cooled to room temperature, an excess of NH<sub>4</sub>PF<sub>6</sub> dissolved in methanol (1 mL) was added and stirring continued for 30 min. The solution was then filtered and concentrated in vacuo until a dark-orange solid formed. The solid was separated by filtration, washed with diethyl ether, and vacuum-dried. The analytically pure product was obtained upon chromatography over neutral alumina with acetonitrile as eluant (*R<sub>f</sub>* = 0.95). Yield, 0.030 g (74%). IR (KBr, cm<sup>-1</sup>):  $\nu(\text{COO})$  1736,  $\nu(\text{PF})$  842. <sup>1</sup>H NMR (CD<sub>3</sub>CN):  $\delta$  (ppm) 8.87 (d, *J* = 2.4 Hz, 1 H), 8.83 (br s, 1 H), 8.75 (m, 2 H), 8.41 (d, *J* = 8.4 Hz, 2 H), 8.27–8.10 (m, 6 H), 7.99–7.87 (m, 10 H), 7.85 (d, *J* = 2.4 Hz, 1 H), 7.80 (s, 1 H), 7.69 (t, *J* = 6.1 Hz, 2 H), 7.62 (d, *J* = 7.3 Hz, 3 H), 7.55 (d, *J* = 8.5 Hz, 3 H), 7.47 (m, 2 H), 7.31 (d, *J* = 7.3 Hz, 2 H), 7.17–7.08 (m, 4 H), 6.96 (m, 4 H), 6.86–6.76 (m, 6 H), 6.66 (vbr s, 4 H), 6.58 (t, *J* = 7.3 Hz, 2 H), 6.38 (t, *J* = 7.3 Hz, 2 H), 5.97 (d, *J* = 8.5 Hz, 2 H), 5.59 (d, *J* = 7.3 Hz, 2 H). Anal. Calcd for C<sub>89</sub>H<sub>58</sub>F<sub>12</sub>Ir<sub>2</sub>N<sub>8</sub>O<sub>2</sub>P<sub>2</sub>: C, 54.94; H, 3.00; N, 5.76. Found: C, 55.11; H, 3.10; N, 5.84.

(24) Demas, J. N.; Crosby, G. A. *J. Phys. Chem.* **1971**, 75, 991.

(25) Nakamaru, K. *Bull. Chem. Soc. Jpn.* **1982**, 55, 2697.

(26) Sprouse, S.; King, K. A.; Spellane, P. J.; Watts, R. J. *J. Am. Chem. Soc.* **1984**, 106, 6647.

(27) Neve, F.; Ghedini, M.; Francescangeli, O.; Campagna, S. *Liq. Cryst.* **1998**, 24, 673.

(28) Neve, F.; Crispini, A.; Campagna, S.; Serroni, S. *Inorg. Chem.* **1999**, 38, 2250.



**[(ppy)<sub>2</sub>Ir( $\mu$ -L-OC(O)-L)Re(CO)<sub>3</sub>Br][PF<sub>6</sub>]<sup>-</sup> (4).** A solid mixture of **2** (0.048 g, 0.037 mmol) and Re(CO)<sub>5</sub>Br (0.015 g, 0.037 mmol) was suspended in dry toluene (20 mL) and heated to reflux under argon for 4 h. The solvent was decanted, and the red sticky solid was redissolved in dichloromethane to afford a red-orange solution. Rotary evaporation of the solvent afforded the crude product. The analytically pure product was obtained as a red-orange solid (0.052 g, 85%) upon chromatography on neutral alumina with a gradient of 3% methanol in dichloromethane as eluant (*R<sub>f</sub>* = 0.7). IR (KBr, cm<sup>-1</sup>):  $\nu$ (CO) 2020, 1919, 1885;  $\nu$ (COO) 1735;  $\nu$ (PF) 842. <sup>1</sup>H NMR (CD<sub>3</sub>CN):  $\delta$  (ppm) 9.13 (m, 1 H), 8.84 (d, *J* = 2.0 Hz, 1 H), 8.77 (br s, 1 H), 8.73 (m, 3 H), 8.40 (d, *J* = 8.8 Hz, 2 H), 8.27 (br t, 1 H), 8.21–8.10 (m, 6 H), 8.05 (d, *J* = 2.0 Hz, 1 H), 7.99–7.83 (m, 6 H), 7.81 (s, 1 H), 7.70–7.60 (m, 7 H), 7.56 (d, *J* = 8.8 Hz, 2 H), 7.46 (m, 2 H), 7.31 (d, *J* = 7.8 Hz, 1 H), 7.17–7.08 (m, 4 H), 6.96 (m, 4 H), 6.83 (t, *J* = 7.4 Hz, 2 H), 6.77 (t, *J* = 7.8 Hz, 4 H), 6.66 (vbr s, 4 H), 6.58 (t, *J* = 7.8 Hz, 2 H), 6.38 (t, *J* = 7.0 Hz, 2 H), 5.97 (d, *J* = 7.0 Hz, 2 H), 5.59 (d, *J* = 7.0 Hz, 2 H). Anal. Calcd for C<sub>70</sub>H<sub>46</sub>BrF<sub>6</sub>IrN<sub>6</sub>O<sub>5</sub>PF<sub>6</sub>: C, 50.82; H, 2.80; N, 5.08. Found: C, 50.17; H, 2.82; N, 5.39.

**[(ppy)<sub>2</sub>Ir( $\mu$ -L-OC(O)-C(O)O-L)Ir(ppy)<sub>2</sub>][PF<sub>6</sub>]<sub>2</sub> (5).** **Method a.** 1,4-Bis(chlorocarbonyl) benzene (0.078 g, 0.038 mmol) was added under nitrogen to a stirred suspension of **1** (0.074 g, 0.076 mmol) in degassed dichloromethane (50 mL). Further addition of a few drops of triethylamine led to the formation of a clear-orange solution. Although a monitoring of the reaction through TLC (SiO<sub>2</sub>, CH<sub>2</sub>Cl<sub>2</sub>/5% MeOH) indicated the disappearance of the chloride within 1 h, stirring was continued at room temperature for 24 h. The solvent was concentrated to a small volume, affording an orange precipitate, which was separated by filtration, washed with methanol and diethyl ether, and vacuum-dried (0.077 g, 96%). IR (KBr, cm<sup>-1</sup>):  $\nu$ (COO) 1736,  $\nu$ (PF) 842. <sup>1</sup>H NMR (CD<sub>3</sub>CN):  $\delta$  (ppm) 8.84 (s, 1 H, H<sup>3'</sup>), 8.76 (d, *J* = 8.2 Hz, 1 H, H<sup>3</sup>), 8.41 (s, 2 H, H<sup>6'</sup>), 8.17 (br t, 1 H, H<sup>4</sup>), 8.13 (d, *J* = 8.7 Hz, 2 H H<sup>a</sup>), 7.99–7.84 (m), 7.81 (s, 1 H, H<sup>5'</sup>), 7.68 (d, *J* = 5.5 Hz, 1 H), 7.62 (d, *J* = 7.6 Hz, 1 H), 7.56 (d, *J* = 8.7 Hz, 2 H, H<sup>b</sup>), 7.47 (m, 1 H), 7.17–7.08 (m, 2 H), 6.95 (m, 2 H), 6.83 (vt, *J* = 7.3 Hz, 1 H), 6.77 (vt, *J* = 7.3, 2 H), 6.66 (vbr s, 2 H), 6.58 (vt, *J* = 7.3 Hz, 1 H), 6.38 (vt, *J* = 7.3 Hz, 1 H), 5.97 (d, *J* = 7.3 Hz, 1 H), 5.59 (d, *J* = 7.3 Hz, 1 H). Anal. Calcd for C<sub>96</sub>H<sub>66</sub>F<sub>12</sub>Ir<sub>2</sub>N<sub>8</sub>O<sub>4</sub>P<sub>2</sub>: C, 55.70; H, 3.21; N, 5.41. Found: C, 55.39; H, 3.13; N, 4.75.

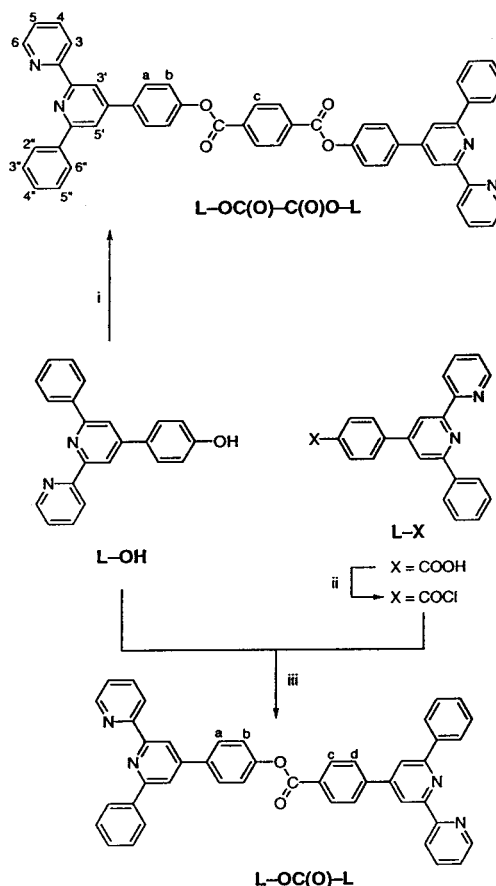
**Method b.** A stirred suspension of [Ir(ppy)<sub>2</sub>Cl]<sub>2</sub> (0.036 g, 0.033 mmol) and L-OC(O)-C(O)O-L (0.025 g, 0.033 mmol) in a CH<sub>2</sub>-Cl<sub>2</sub>/MeOH (10 mL/12 mL) mixture was heated under reflux conditions for 4 h. After the resulting orange solution was cooled to room temperature, a methanolic solution (1 mL) of NH<sub>4</sub>PF<sub>6</sub> (10 equiv based on the ligand) was added to it and stirring continued for 30 min. Partial evaporation of the solvent under reduced pressure afforded the product as an orange solid, which was filtered off, washed with methanol and diethyl ether, and dried in vacuo (0.057 g, 82%). Upon analysis, the product turned out to be identical to that obtained by method a.

**[ReBr(CO)<sub>3</sub>(L-COOH)] (6).** Re(CO)<sub>5</sub>Br (0.069 g, 0.170 mmol) and L-COOH (0.060 g, 0.170 mmol) were stirred for 4 h under argon in refluxing dry toluene (15 mL). The resulting bright-yellow solid was collected and washed with diethyl ether and hexane before drying in vacuo (0.114 g, 95%). IR (KBr, cm<sup>-1</sup>):  $\nu$ (CO) 2023, 1921, 1902;  $\nu$ -(COOH) 1720. <sup>1</sup>H NMR (CD<sub>3</sub>CN-CDCl<sub>3</sub>):  $\delta$  (ppm) 9.11 (br d, 1 H, H<sup>6'</sup>), 8.71 (br s, 1 H, H<sup>3'</sup>), 8.67 (d, *J* = 8.5 Hz, 1 H, H<sup>3</sup>), 8.24 (br t, 1 H, H<sup>4</sup>), 8.20 (d, *J* = 8.5 Hz, 2 H, H<sup>a</sup>), 8.07 (d, *J* = 8.5 Hz, H<sup>b</sup>), 7.97 (d, *J* = 2.4 Hz, 1 H, H<sup>5'</sup>), 7.71–7.58 (m, 6 H, H<sup>2',6'</sup> + H<sup>3',4',5'</sup> + H<sup>5</sup>). Anal. Calcd for C<sub>26</sub>H<sub>14</sub>BrIrN<sub>2</sub>O<sub>5</sub>Re: C, 44.45; H, 2.30; N, 3.99. Found: C, 44.78; H, 2.41; N, 4.04.

## Results

Assembling photoactive polymetallic species can be a lengthy process, especially when heteronuclear or asymmetric assemblies must be generated.<sup>1–6</sup> Even in the simplest case, i.e., for bimetallic species, most synthetic methods are based on a stepwise approach that ensures control of the target species.<sup>29–31</sup>

**Scheme 1.** Synthesis of the Ligands<sup>a</sup>



<sup>a</sup> Reagents: (i) 1,4-(COCl)<sub>2</sub>C<sub>6</sub>H<sub>4</sub> (0.5 equiv), NEt<sub>3</sub>; (ii) SOCl<sub>2</sub>; (iii) NEt<sub>3</sub>.

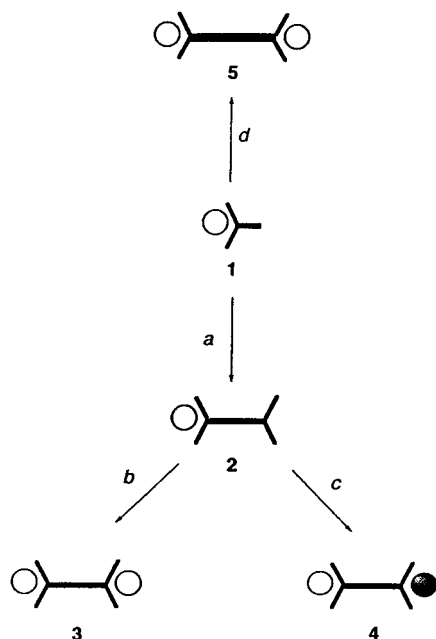
To prepare Ir-based bimetallic complexes, we followed two different strategies that both rely on a common building block. From our recent studies,<sup>28</sup> it is known that the complex [(ppy)<sub>2</sub>Ir(L-OH)][PF<sub>6</sub>]<sup>-</sup> (**1**, Chart 1) (ppy = 2-phenylpyridine anion; L-OH = 4'-(4-hydroxyphenyl)-6'-phenyl-2,2'-bipyridine) has two main characteristics: (i) it is a good luminophore and (ii) it bears a reactive OH group at the periphery of a coordinated ligand. By means of **1**, construction of the bimetallic species can go either through a single-step reaction to generate symmetric species or through a multistep process that leads to asymmetric species. In the latter case, the key role would be played by the complex ligand **2** (Chart 1), a potential candidate for luminescent dyads<sup>32</sup> or triads.<sup>33</sup>

**Syntheses of the Ligands.** The syntheses of the asymmetric L-OC(O)-L and symmetric L-OC(O)-C(O)O-L multi-nucleating ligands based on the 6'-phenyl-2,2'-bipyridine functionality are reported in Scheme 1. In both cases the synthesis is rather straightforward, implying a condensation under mild conditions of an acid chloride with a phenolic functional group in the presence of triethylamine as a base. The ligands were obtained in very good yield after purification by column chromatography and characterized by FT-IR and <sup>1</sup>H NMR spectroscopies.

- (30) Whittle, B.; Everest, N. S.; Howard, C.; Ward, M. D. *Inorg. Chem.* **1995**, *34*, 2025.
- (31) Paw, W.; Eisenberg, R. *Inorg. Chem.* **1997**, *36*, 2287.
- (32) Aspley, C. J.; Lindsay Smith, J. R.; Perutz, R. N. *Chem. Commun.* **1999**, 2269.
- (33) Barigelli, F.; Flamigni, L.; Calogero, G.; Hammarström, L.; Sauvage, J.-P.; Collin, J.-P. *Chem. Commun.* **1998**, 2333.

(29) Constable, E. C.; Cargill Thompson, A. M. W.; Herveson, P.; Macko, L.; Zehnder, M. *Chem. Eur. J.* **1995**, *1*, 360.

Scheme 2



Although the free ligands were synthesized and fully characterized for the first time in the present study, they were not used for the preparation of the metal complexes reported here (except in one case). Nevertheless, their characterization was useful to allow the subsequent characterization of the metal species.

**Syntheses of the Metal Complexes.** As mentioned above, our synthetic strategy for the preparation of multimetallic species took advantage of the available complex  $[\text{Ir}(\text{ppy})_2(\text{L}-\text{OH})][\text{PF}_6]$  (**1**) (Chart 1), which possesses a reactive functional group at the periphery of the chelating  $\text{L}-\text{OH}$  ligand. Condensation of the phenolic function of **1** with the chlorocarbonyl group of the  $\text{L}-\text{COCl}$  derivative (ad hoc prepared from  $\text{L}-\text{COOH}$ ) exclusively led to the formation of  $[\text{Ir}(\text{ppy})_2(\text{L}-\text{OC}(\text{O})-\text{L})][\text{PF}_6]$  (**2**) (Scheme 2, route a), thus affording a mononuclear species that contains a free bipyridyl binding site belonging to the ligand  $\text{L}-\text{OC}(\text{O})-\text{L}$  formed in situ.

Complex **2**, which is air-stable and fairly soluble in common organic solvents, is therefore able to behave as a complex ligand, and virtually any type of bimetallic system can be assembled provided the second metal center has neither severe steric constraints nor high inertness. Although in principle complex **2** may behave as a mono-, bi-,<sup>28,34</sup> or tridentate complex ligand,<sup>27,35,36</sup> we chose to pursue its more predictable reactivity as donor of a bipyridyl fragment. The reaction of **2** with 0.5 equiv of  $[\text{Ir}(\text{ppy})_2\text{Cl}]_2$  followed by metathesis with  $\text{NH}_4\text{PF}_6$  (Scheme 2, route b) readily afforded the homometallic species  $[(\text{ppy})_2\text{Ir}(\mu-\text{L}-\text{OC}(\text{O})-\text{L})\text{Ir}(\text{ppy})_2][\text{PF}_6]_2$  (**3**). On the other hand, the heterometallic species  $[(\text{ppy})_2\text{Ir}(\mu-\text{L}-\text{OC}(\text{O})-\text{L})\text{Re}(\text{CO})_3\text{Br}][\text{PF}_6]$  (**4**) could be obtained by reaction of **1** and  $\text{Re}(\text{CO})_5\text{Br}$  following well-known procedures<sup>37–39</sup> (Scheme 2, route c). Prepared in a similar manner, the complex  $[\text{Re}(\text{CO})_3(\text{L}-\text{COOH})]$  (**6**) was intended to serve as a model in the interpretation of the photophysical and redox behavior of **4**.

Besides, **6** was also instrumental in the assignment of the stereochemistry of the Re site in complex **4**. The IR spectra of both **4** and **6** show three intense absorption bands in the spectral region characteristic of terminal carbonyl ligands ( $2030\text{--}1880\text{ cm}^{-1}$ ), a feature that is in agreement with a facial arrangement of the carbonyl groups of the  $\text{Re}(\text{CO})_3$  fragment.<sup>40</sup> This finding rules out the possibility for a cyclometalating, tridentate bonding mode of the L moiety, since involvement of a metalated phenyl group would likely lead to the formation of a  $\text{Re}(\text{I})$  octahedral complex with meridional configuration. The absence of a Re cyclometalated L moiety in **6** (and by extension in **4**) was also proved by the  $^1\text{H}$  NMR characterization of the complex, which revealed the presence of an uncoordinated phenyl group. Finally, the coordination mode of the ditopic  $\text{L}-\text{OC}(\text{O})-\text{L}$  ligand in **2–4** is always N,N to both Ir and Re. For the former, the metal environment is barely that of complex **1**, which has been previously defined.<sup>28</sup>

The  $^1\text{H}$  NMR spectra of **2–4** were recorded in acetonitrile- $d_3$ , affording aromatic regions very rich in signals. Although no effort has been made to fully assign the spectra, two pairs of resonances can be easily followed for an indication of the second metal binding. These refer to the  $\text{H}^{3'}$  and  $\text{H}^{5'}$  protons of the central pyridine ring of both termini of the  $\text{L}-\text{OC}(\text{O})-\text{L}$  ligand. When uncoordinated (as in **2**), the signals of the free L terminus are observed at  $\delta$  8.74 and 8.25, respectively (see Experimental Section). Metal coordination triggers downfield and upfield shifts to  $\delta$  8.80 and 7.82 for **3** and  $\delta$  8.77 and 8.05 for **4**. On the other hand, the remaining pair of signals, which we assign to the  $\text{H}^{3'}$  and  $\text{H}^{5'}$  protons of the pyridine always bound to iridium, are displayed around  $\delta$  8.80 and 7.80 for all three complexes, revealing a common chemical environment.

Complex **1** was also effective in the formation of symmetric bimetallic species. The room-temperature coupling of **1** with 0.5 equiv of terephthaloyl chloride followed by exchange with  $\text{NH}_4\text{PF}_6$  (Scheme 2, route d) led to the dicationic species **5**, in a way that involved the formation of both a new bridging ligand and the bimetallic assembly. Interestingly, complex **5** is the only member of the series of bimetallic species reported here that can be synthesized by an alternative, more conventional method. Thus, the direct reaction of the ligand  $\text{L}-\text{OC}(\text{O})-\text{C}(\text{O})\text{O}-\text{L}$  with the dimer  $[\text{Ir}(\text{ppy})_2\text{Cl}]_2$  under reflux conditions (followed by exchange with excess  $\text{NH}_4\text{PF}_6$  at room temperature) also led to the formation of **5** in good yield. Attempts to obtain Ir-based trimetallic species through the coupling of **1** with the electrophile 1,3,5-tris(chlorocarbonyl)benzene<sup>41</sup> were unsuccessful. The reaction gave rise to a complex mixture of products that could not be separated and identified.

**Redox Behavior and Spectroscopic and Photophysical Properties.** The absorption spectra of all the novel compounds exhibit moderately intense absorption in the visible region ( $\epsilon$  in the range  $10^3\text{--}10^4\text{ M}^{-1}\text{ cm}^{-1}$ ) and a strong absorption in the UV region ( $\lambda_{\text{max}}$  at about 270 nm,  $\epsilon$  in the range  $10^4\text{--}10^5\text{ M}^{-1}\text{ cm}^{-1}$ ). They also show a broad tail that extends toward the red region. All the compounds exhibit one irreversible oxidation process at about +1.20 V vs SCE, and **4** also shows an additional irreversible oxidation process at +1.34 V. The processes concerning **2**, **4**, and **6** are monoelectronic, whereas the oxidation processes of the diiridium species **3** and **5** are bielectronic in nature. The complexes also show reversible reduction processes in the potential window investigated ( $<1.80\text{ V}$ ).

(34) Neve, F.; Crispini, A. *Eur. J. Inorg. Chem.* **2000**, 1039.

(35) Neve, F.; Ghedini, M.; Crispini, A. *Chem. Commun.* **1996**, 2463.

(36) Neve, F.; Crispini, A.; Campagna, S. *Inorg. Chem.* **1997**, *36*, 6150.

(37) Abel, E. W.; Wilkinson, G. *J. Chem. Soc.* **1959**, 1501.

(38) Wrighton, M. S.; Morse, D. L. *J. Am. Chem. Soc.* **1974**, *96*, 998.

(39) Juris, A.; Campagna, S.; Bidd, I.; Lehn, J.-M.; Ziessel, R. *Inorg. Chem.* **1988**, *27*, 4007.

(40) Stor, G. J.; Morrison, S. L.; Stufkens, D. J.; Oskam, A. *Organometallics* **1994**, *13*, 2641.

(41) Davies, P. J.; Grove, D. M.; van Koten, G. *Organometallics* **1997**, *16*, 800.

**Table 1.** Half-Wave Potentials in Argon-Purged Acetonitrile Solution, 298 K<sup>a</sup>

compound	$E_{1/2}(\text{ox})$ , <sup>b</sup> V vs SCE	$E_{1/2}(\text{red})$ , V vs SCE
<b>2</b> $[\text{Ir}(\text{ppy})_2(\text{L}-\text{OC}(\text{O})-\text{L})]^+$	+1.19 [1]	-1.35 [1]; -1.68 [1]
<b>3</b> $[(\text{ppy})_2\text{Ir}(\mu\text{-L}-\text{OC}(\text{O})-\text{L})\text{Ir}(\text{ppy})_2]^{2+}$	+1.18 [2]	-1.24 [1]
<b>4</b> $[(\text{ppy})_2\text{Ir}(\mu\text{-L}-\text{OC}(\text{O})-\text{L})\text{Re}(\text{CO})_3\text{Br}]^+$	+1.19 [1]; +1.34 [1]	-1.20 [1]; -1.35 [1]
<b>5</b> $[(\text{ppy})_2\text{Ir}(\mu\text{-L}-\text{OC}(\text{O})-(\text{O})\text{CO}-\text{L})\text{Ir}(\text{ppy})_2]^{2+}$	+1.19 [2]	-1.35 [1]; -1.53 [1]
<b>6</b> $[\text{Re}(\text{CO})_3(\text{L}-\text{COOH})\text{Br}]$	+1.34 [1]	-1.25 [1]

<sup>a</sup> The number of exchanged electrons is reported in brackets. <sup>b</sup> Irreversible process. In this case, the value reported is the dpv peak.

**Table 2.** Spectroscopic and Photophysical Data<sup>a</sup>

compound	absorption <sup>b</sup> $\lambda_{\text{max}}$ , nm ( $\epsilon$ , $\text{M}^{-1}\text{cm}^{-1}$ )	luminescence, 298 K						lumin, <sup>d</sup> 77 K	
		$\lambda_{\text{max}}$ , nm <sup>b</sup>	$\tau$ , ns <sup>b</sup>	$\Phi$ <sup>b</sup>	$\lambda_{\text{max}}$ , <sup>c</sup> nm	$\tau$ , <sup>c</sup> ns	$\Phi$ <sup>c</sup>	$\lambda_{\text{max}}$ , nm	$\tau$ , $\mu\text{s}$
<b>2</b> $[\text{Ir}(\text{ppy})_2(\text{L}-\text{OC}(\text{O})-\text{L})]^+$	270 (92500) 377 (7300)	633	75	0.016	619	192	0.059	545	3.6
<b>3</b> $[(\text{ppy})_2\text{Ir}(\mu\text{-L}-\text{OC}(\text{O})-\text{L})\text{Ir}(\text{ppy})_2]^{2+}$	269 (117700) 380 (18500)	646	65	0.006	638	167	0.040	552	3.5
<b>4</b> $[(\text{ppy})_2\text{Ir}(\mu\text{-L}-\text{OC}(\text{O})-\text{L})\text{Re}(\text{CO})_3\text{Br}]^+$	271 (83400) 378 (12800)	636	62	0.005	623	169	0.025 <sup>e</sup>	550	3.3
<b>5</b> $[(\text{ppy})_2\text{Ir}(\mu\text{-L}-\text{OC}(\text{O})-(\text{O})\text{CO}-\text{L})\text{Ir}(\text{ppy})_2]^{2+}$	269 (120500) 380 (15900)	631	69	0.007	620	188	0.045	548	3.6
<b>6</b> $[\text{Re}(\text{CO})_3(\text{L}-\text{COOH})\text{Br}]$	270 (34200) 382 (4400)	643	35	0.002	655	46	0.004	562	4.8

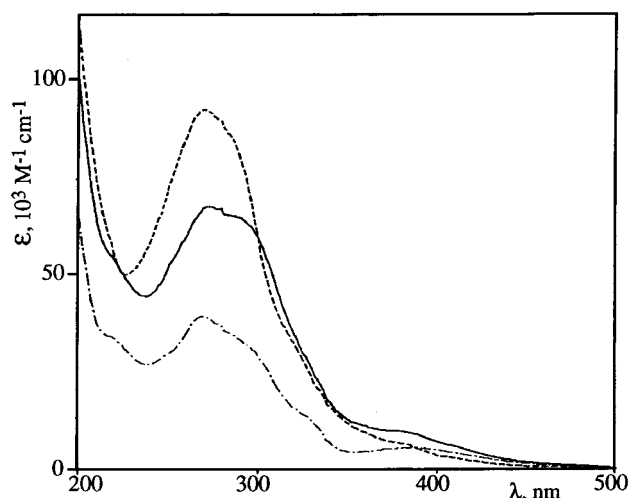
<sup>a</sup> For the absorption, the maxima (or shoulders) of the spin-allowed LC and MLCT bands are given. <sup>b</sup> In air-equilibrated  $\text{CH}_3\text{CN}$ . <sup>c</sup> In air-equilibrated  $\text{CH}_2\text{Cl}_2$ . <sup>d</sup> In butyronitrile. <sup>e</sup> This quantum yield is excitation wavelength dependent (see text). The one reported is the average value.

All the compounds are luminescent both at room temperature in acetonitrile and in dichloromethane fluid solution and at 77 K in butyronitrile rigid matrix. The luminescence maxima are solvent-dependent; they are shifted to the blue on passing from acetonitrile to dichloromethane solution, except for **6** which exhibits the reverse effect. The luminescence spectra always show relatively broad bands. A vibrational structure is visible as a shoulder in the red tail of the main band, especially at 77 K. Luminescence decays are monoexponential and are in the microsecond time scale at 77 K and 1 or 2 orders of magnitude shorter at 298 K. For all the complexes, luminescence lifetimes and quantum yields increase on passing from acetonitrile to dichloromethane. The luminescence properties are in all cases independent of excitation wavelength (between 320 and 420 nm) when experimental uncertainty is taken into account, with the exception of the luminescence quantum yield of **4** in dichloromethane (see Discussion). Table 1 is a listing of the redox data, while the spectroscopic and photophysical data are gathered in Table 2. Figure 1 shows the absorption spectra of **2**, **4**, and **6** in acetonitrile, and Figure 2 displays the emission spectra of **4** in acetonitrile and dichloromethane fluid solutions at room temperature and in butyronitrile at 77 K.

## Discussion

The spectroscopic and photophysical properties and the redox behavior of transition metal complexes and organometallic compounds are usually discussed with the assumption that the ground state, as well as the excited and redox states, can be described by a localized molecular orbital configuration.<sup>42,43</sup> Within this framework, the various spectroscopic transitions and excited states are classified as metal-centered (MC), ligand-centered (LC), or charge-transfer (either metal-to-ligand, MLCT, or ligand-to-metal, LMCT) and the oxidation and reduction processes are classified as metal- or ligand-centered.<sup>42–44</sup>

- (42) De Armond, M. K.; Carlin, C. M. *Coord. Chem. Rev.* **1981**, 36, 325.  
 (43) Juris, A.; Balzani, V.; Barigelletti, F.; Campagna, S.; Belser, P.; von Zelewsky, A. *Coord. Chem. Rev.* **1988**, 84, 85.  
 (44) Maestri, M.; Balzani, V.; Deuschel-Cornioley, C.; von Zelewsky, A. *Adv. Photochem.* **1992**, 17, 1.

**Figure 1.** Absorption spectra of complexes **2** (dashed line), **4** (solid line), and **6** (dashed-dotted line) in acetonitrile at room temperature.

Recently, other particular types of orbitals (and states) have also been proposed to rationalize the spectroscopic and electrochemical properties of metal compounds containing strong electron-donor ligands. For example, a covalent metal–C<sup>–</sup>  $\sigma$ -bonding (or metal–Si<sup>–</sup>  $\sigma$ -bonding) orbital has been identified as the orbital involved in the oxidation process and the lowest-lying charge-transfer excited state in Ir(III) cyclometalated compounds.<sup>45–47</sup> The excited states derived from these  $\sigma$ -bonding orbitals are usually termed  $\sigma$ -bond to ligand charge-transfer (SBLCT)<sup>46,47</sup> or more generally ligand-to-ligand charge transfer (LLCT).<sup>48</sup>

The species investigated here can be viewed as multicomponent compounds. Even the bridging ligands may be viewed as multicomponent, segmented species in that their chelating

- (45) Djurovich, P. I.; Watts, R. J. *Inorg. Chem.* **1993**, 32, 4681.  
 (46) Didier, P.; Ortman, L.; Kirsch-DeMesmaeker, A.; Watts, R. J. *Inorg. Chem.* **1993**, 32, 5239.  
 (47) Serroni, S.; Juris, A.; Campagna, S.; Venturi, M.; Denti, G.; Balzani, V. *J. Am. Chem. Soc.* **1994**, 116, 9086.  
 (48) Vogler, A. In *Photoinduced Electron Transfer*; Fox, M. A., Chanon, M., Eds.; Elsevier: Amsterdam, 1988; p 179.



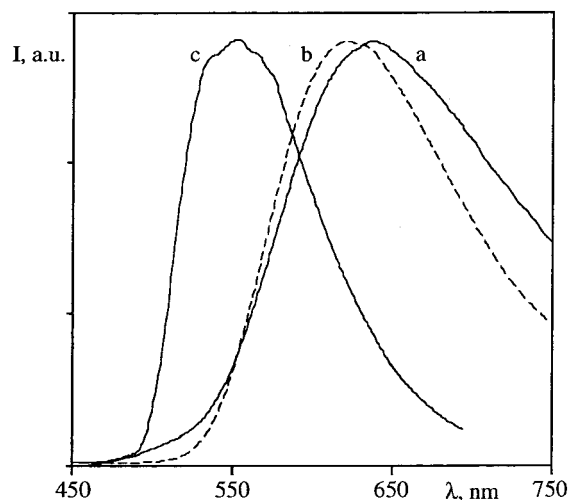


**Figure 2.** Corrected luminescence spectra of **4** in acetonitrile (a) and dichloromethane (b, dashed line) fluid solutions at room temperature and in butyronitrile (c) at 77 K.

sites are connected to each other by ester linkages. To simplify the discussion, we will make extensive use of this picture.

**Redox Behavior.** As mentioned above, oxidations of  $d^6$  metal complexes containing polypyridine and cyclometalating ligands are usually metal-centered or may involve orbitals that receive partial contributions from  $\sigma$  bonds. Generally, pure metal-centered oxidations are reversible, and the contribution of ligand-centered orbitals via the  $\sigma$  bond leads to irreversible processes. In light of the irreversibility of the oxidation processes exhibited by the complexes studied here (Table 1), we assign such processes to orbitals that receive contributions from  $M-C^-\sigma$  bonds.

It is interesting to compare the oxidation behavior of **2** and **5**, which contain identical redox centers, leaving aside the second coordination site of the bridging ligand. Because of its bielectronic nature (Table 1), the oxidation of **5** is assigned to two simultaneous, one-electron processes involving the two metal-based subunits. This indicates that the electronic interaction between the two identical redox sites of **5** across the bridge, usually inferred by the splitting of the redox processes in symmetric dinuclear complexes, is negligible from an electrochemical viewpoint. The identical potentials of the oxidation processes of **2** and **5** also suggest that the coordination through the second chelating site of the bridging ligand does not significantly affect the electronic properties of the other redox site. Even the oxidation of **3** can be assigned to simultaneous one-electron processes involving the two metal-based subunits, although in principle the two redox centers are different, as a consequence of the bridge asymmetry. Actually, we may consider the  $L-OC(O)-L$  bridging ligand as being formed by two subunits, one in which the phenylbipyridine chelating site bears an oxycarbonyl group as substituent (hereafter  $L-OC(O)$ ) and the other in which the substituent is a carboxyl group (hereafter  $L-C(O)O$ ) (see Figure 3). Since  $L-C(O)O$  is a slightly better electron-acceptor ligand than  $L-OC(O)$ , one might expect that the redox center  $\{(ppy)_2Ir(L-C(O)O)\}$  is oxidized at more positive potentials than the  $\{(ppy)_2Ir(L-OC(O))\}$  fragment. In fact, the simultaneous oxidation of the two redox centers of **3** indicates that this difference does not have a sizable effect. As far as **4** is concerned, its first oxidation process is safely assigned to the iridium center and the second one to the rhenium center, on the basis of the potential values of the oxidations reported in Table 1.

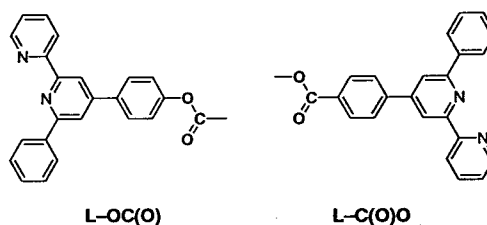


**Figure 3.** Two chelating subunits of the  $L-OC(O)-L$  bridging ligand (see text).

For the sake of simplicity, we will start the discussion on the reduction processes from complex **2** (Table 1). The first reduction process of this compound may be assigned to the reduction of the coordinated  $L-OC(O)$  moiety of the  $L-OC(O)-L$  ligand, and the subsequent reduction may be assigned to the uncoordinated polypyridine moiety of the same ligand. This is based on the reported potential values for the reduction processes of the coordinated ppy ligands, which are known to be more negative than  $-1.80$  V,<sup>44</sup> and on the fact that coordinated polypyridines are reduced at less negative potentials than uncoordinated ones. Compound **5** contains the same type of coordinated site that is present in **2**. Therefore, the first reduction of **5**, occurring at the same potential as the first reduction of **2**, is also assigned to either one of the  $L-OC(O)$  moieties of the  $L-OC(O)-C(O)O-L$  bridge. The second reduction is attributed to the remaining  $L-OC(O)$  site of the same ligand. Because reduction is essentially bpy-centered, the monoreduced species can be regarded as a mixed-valence, (bis-phenyl-bpy<sup>-</sup>)-S-(bis-phenyl-bpy) species, where S represents the dicarboxylate phenyl spacer (see Chart 1). To evaluate the stability of the mixed-valence species and as a consequence the electronic interaction between the sites, the comproportionation constant  $K_c$  is useful.<sup>49</sup> This can be obtained by the equation (at 298 K)  $K_c = \exp(\Delta E/25.69)$ , where  $\Delta E$  corresponds to the difference between the first and second redox potentials in millivolts. From the reported values, a  $K_c$  value of 1100 is obtained, which indicates a significant interaction between the two moieties of the bridging ligand across the dicarboxylate phenyl spacer. This looks somewhat surprising, given the oxidation properties of **5** (see above), which suggest a negligible interaction between the metal ions across the bridging ligand. However, the redox-active sites involved in the reduction process are closer to one another than those involved in the oxidation process. Actually, the orbitals involved in the reduction processes, mainly centered on the bipyridine moieties, are also most likely partially extended to the phenyl rings directly connected to the carboxylate spacer, whereas the oxidation processes involve  $Ir-C^-\sigma$ -bonding orbitals where peripheral ligands have a role. Such differences justify the observed behavior as far as the interaction between redox sites is concerned, when Coulombic effects and the mechanism for superexchange-mediated coupling between the redox-active sites<sup>49</sup> are taken into account.

The reduction process of **3** is assigned to the  $L-C(O)O$  coordinated moiety of the bridge. This moiety is a better electron acceptor than  $L-OC(O)$ , and this agrees with the less negative potential of the process with respect to the first reduction processes of **2** and **5**. Because of adsorption on the electrode, further investigation of the reduction behavior of **3** was prevented. Reduction of **6** is assigned straightforwardly to the polypyridine ligand (the only reduction site of this complex),

(49) Giuffrida, G.; Campagna, S. *Coord. Chem. Rev.* **1994**, 135–136, 517 and references therein.



and this assignment allows the attribution of the first reduction process of **4** to the  $\text{L}-\text{C}(\text{O})\text{O}$  moiety coordinated to  $\text{Re}(\text{I})$  and of the second reduction to the Ir-coordinated moiety of the bridge (Table 1).

**Absorption Spectra.** On the basis of literature data,<sup>26,28,44–47</sup> the moderate absorption bands exhibiting a maximum (or most often a shoulder) at about 380 nm, which is present in all the new complexes, can be attributed to spin-allowed MLCT transitions involving the polypyridine ligands, whereas the strong absorption peaks at about 270 nm can be attributed to spin-allowed LC transitions (Table 2, Figure 1). This attribution also indicates that LC transitions involving ppy and the bridging ligands occur in the same energy region. The tail toward the red region (Figure 1), which is present in all the complexes (maxima or shoulders at about 470 nm), is attributed to spin-forbidden MLCT transitions, which steal intensity from the spin-allowed bands because of the strong spin–orbit coupling induced by the heavy metals.

From the extinction coefficients reported in Table 2, it is clear that the absorption spectra are essentially additive. For example, the molar absorption coefficient of the MLCT absorption of **5** is almost twice that of the corresponding MLCT band in **2**, in which a metal ion is missing, whereas the LC band is only slightly enhanced because of the presence of two additional ppy ligands in **5**. While the LC extinction coefficients of **5** and **3** are roughly the same (only a slight difference in the bridge is present), the MLCT band is significantly more intense in **3**. This suggests that the  $\text{Ir} \rightarrow \text{L}-\text{C}(\text{O})\text{O}$  charge-transfer (CT) transition has a stronger oscillator strength than the  $\text{Ir} \rightarrow \text{L}-\text{OC}(\text{O})$  CT transition. Finally, both the LC and MLCT bands of **6** are less intense than those of the other species, including **2**, suggesting that  $\text{Re} \rightarrow \text{L}-\text{OC}(\text{O})$  CT transition has a lower oscillator strength than the Ir-based CT ones. This also explains the extinction coefficient values of the MLCT and LC bands of **4**, which are lower than the corresponding bands of the other dinuclear species. As we will see later, the differences in molar absorptivities of the different subunits will be very important in determining the luminescence properties of the various compounds.

**Luminescence Properties.** The luminescence of all the complexes studied here (Table 2, Figure 2) can be safely attributed to <sup>3</sup>MLCT excited states involving the polypyridine ligands, on the basis of spectral shape, emission energies, lifetimes, and quantum yields.<sup>16–21,26,28,44–47</sup> The red shift of the emission spectra of the Ir-based complexes on passing from dichloromethane to acetonitrile also agrees with this assignment in that the more polar acetonitrile stabilizes the MLCT levels with respect to the ground state because of the more polar character of the former levels compared to the latter. The reverse behavior of the rhenium species (Table 2) is also in line with expectation in that it is well-known that for  $\text{Re}(\text{I})$  tricarbonyl luminophores the excited state is less polar than the ground state, so these species show a different solvatochromic effect compared with  $\text{Ir}(\text{III})$  (and also  $\text{Ru}(\text{II})$  and  $\text{Os}(\text{II})$ ) polypyridine compounds.<sup>37–39</sup> In all cases, luminescence lifetimes and quantum yields are lower in acetonitrile because this solvent accelerates radiationless transitions with respect to dichloromethane. The blue shift of the emission spectra on passing from fluid solution at room temperature to rigid matrix at 77 K is also typical of charge-transfer emitters, as a consequence of the absence of the excited-state stabilization due to solvent reorganization processes, which are hampered in a rigid matrix.<sup>50</sup>

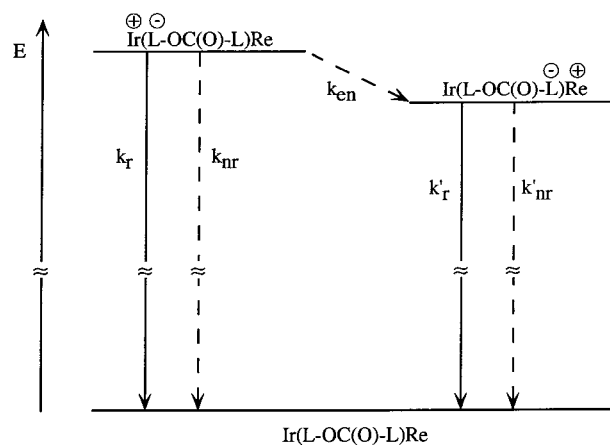


**Figure 4.** Schematic energy level diagram of **4**. Solid and dashed lines represent radiative and radiationless transitions, respectively. The peripheral ligands and the effective charges of the complexes are not reported for convenience.

One of our aims in designing and studying these species was to clarify whether photoinduced energy transfer across the ester-linked multichelating bridging ligands could occur in compounds containing different chromophores. Compounds **3** and **4** are indeed suitable in this regard in that each of them contains two intrinsically emitting chromophores with MLCT excited states that are different in energy; **3** contains an  $\text{Ir} \rightarrow \text{L}-\text{OC}(\text{O})$  CT excited state (hereafter  $\text{MLCT}_1$ ) together with an  $\text{Ir} \rightarrow \text{L}-\text{C}(\text{O})\text{O}$  CT level (hereafter  $\text{MLCT}_2$ ). The  $\text{MLCT}_1$  level is also present in **4** in which a  $\text{Re} \rightarrow \text{L}-\text{C}(\text{O})\text{O}$  CT level (hereafter  $\text{MLCT}_3$ ) is also present. On the basis of the redox properties of the various subunits and on the photophysical properties of **2**, **5**, and **6**, the excited-state energy order is  $\text{MLCT}_3 < \text{MLCT}_2 < \text{MLCT}_1$ , and as a consequence, exoergic photoinduced energy transfer from  $\text{MLCT}_1$  to  $\text{MLCT}_2$  in **3** and from  $\text{MLCT}_1$  to  $\text{MLCT}_3$  in **4** could occur, although in both cases the driving force is small.<sup>51</sup> The situation for complex **4** is schematized in Figure 4.

The discussion on the energy-transfer processes will proceed starting from compound **4**. A cursory look at Table 2 indicates that the luminescence properties of **4** are dominated by the  $\text{MLCT}_1$  level of the upper-lying luminophore both in rigid matrix and in fluid solution, so energy transfer from  $\text{MLCT}_1$  to the lower-lying  $\text{MLCT}_3$  level seems to occur with low efficiency. By comparison of the absorption and luminescence properties of **2** and **6**, it appears that the Ir-based chromophore is both a better absorber and luminophore than the Re-based one, and this also explains why the luminescence properties of **4** look Ir-based. Following this consideration, it could be proposed that the two chromophores of **4** are essentially noninteracting. A useful hint in this regard is the dependence of the luminescence quantum yield ( $\Phi$ ) of **4** in dichloromethane on the excitation wavelength. In fact, the  $\Phi$  value for **4** in dichloromethane is 0.030 for  $\lambda_{\text{exc}} = 360$  nm (where the

(51) It is noted that there is an apparent lack of correlation between spectroscopic and redox properties in **4**, for which the HOMO involves (from redox data, Table 1) an Ir-based orbital while the lowest-lying MLCT excited state involves (on the basis of the photophysical properties of the parent mononuclear species **2** and **6**; Table 2) a Re-based orbital. It should be recalled that the spectroscopic/electrochemical relationship is usually followed in mononuclear species, but it loses its meaning in multicomponent (supramolecular) systems in which the HOMO and LUMO of the compound can belong to different subunits. In **4**, the LUMO is centered on the polypyridine moiety of the bridging ligand connected to the  $\text{Re}(\text{I})$  center, and as a consequence, it is not surprising that the MLCT level involving this metal center is lower-lying than the MLCT level involving the Ir center, where the HOMO is localized.

(50) Chen, P.; Meyer, T. J. *Chem. Rev.* **1998**, 98, 1439 and references therein.

compound is predominantly excited in the Ir center over the Re center; see Figure 1), and it decreases to 0.024 for  $\lambda_{\text{exc}} = 395$  nm (where the two centers are approximately equally excited) and to 0.020 for  $\lambda_{\text{exc}} = 410$  nm (where the Re center should be predominantly excited). This suggests that energy transfer between the chromophores is not an efficient process. However, on the basis of the quantum yields of the parent mononuclear species **2** and **6** (Table 2), the difference in quantum yields on excitation wavelength should be much larger if energy transfer were totally inefficient, so partial energy transfer between the chromophores in **4** seems to take place. The analogous experiment in acetonitrile is not equally useful because the differences in quantum yields ( $\Phi = 0.0055$  for  $\lambda_{\text{exc}} = 360$  nm and  $\Phi = 0.0042$  for  $\lambda_{\text{exc}} = 410$  nm) are close to the experimental errors (20%, as given in the Experimental Section), as also expected because of the closer quantum yields of the two subunits (see Table 2).

In the absence of energy transfer, in principle the emission spectra should be wavelength-dependent and the luminescence decays should be multiexponential. This disagrees with our findings (see Results and data collected in Table 2). However, the absorption spectra of the two components are very similar to each other in shape, with the Ir-based chromophore absorbing more efficiently, and this makes excitation spectroscopy hardly capable of identifying multiple emissions. Moreover, the different emission outputs<sup>52</sup> made it experimentally difficult to look for a minor component in the luminescence decay. However, as also pointed out by one of the referees, two decays characterized by a 1:10 preexponential factor difference and with a difference in lifetime larger than 4 (as should be the case for the two emitting levels of **4** in dichloromethane, on the basis of the data of the parent complexes **2** and **6**) should be detectable. Because this is not the case, most likely partial energy transfer takes place, smearing out the lifetime differences and making detection of the second component much more difficult.

As far as compound **3** is concerned, the luminescence spectra of this species both in rigid matrix and in fluid solution are significantly red-shifted with respect to **2** and **5**, in which only the MLCT<sub>1</sub> luminophore is present. This suggests that the emission of **3** is dominated by the MLCT<sub>2</sub> luminophore. This would also imply energy transfer from MLCT<sub>1</sub> to MLCT<sub>2</sub> across the bridge. However, comparison of the luminescence properties of **3** with those of the mononuclear complex [Ir(ppy)<sub>2</sub>(cpbpy)]<sup>+</sup> (**7**, cpbpy = 4'-(4-carboxyphenyl)-6'-2,2'-bipyridine; data in nitrogen-saturated acetonitrile at room temperature are  $\lambda_{\text{max}} = 660$  nm,  $\tau = 125$  ns,  $\Phi = 0.017$ ; data for alcoholic matrix at 77 K are  $\lambda_{\text{max}} = 565$  nm,  $\tau = 3.3$   $\mu$ s),<sup>28</sup> in which an excited state very similar to MLCT<sub>2</sub> is present, indicates that the emission of **3** does not occur from a pure MLCT<sub>2</sub> level. A clear-cut statement indeed is difficult to make. In principle, three cases may occur: (a) the two chromophores are only weakly interacting, with energy transfer (if any) occurring only to a minor extent so that each chromophore essentially contributes almost independently to the emission properties, as it seems to be the case for **4**; (b) complete energy transfer occurs and the luminescence properties are dominated by the MLCT<sub>2</sub> luminophore; (c) fast equilibration between the two emitting states occurs (this would imply noticeable interaction) and the

luminescence properties are typical of the coupled systems. The luminescence lifetimes and quantum yields are not useful in clarifying the problem; intrinsic luminescence lifetimes of the two "isolated" chromophores are expected to be very similar so that single-photon-counting experiments cannot show the presence of multiexponential decays, and the same occurs for the quantum yields. In fact, the luminescence quantum yield for **3** is independent of the excitation wavelength both in acetonitrile and in dichloromethane solution within the experimental error because of the similarity in the quantum yields expected for the "isolated" chromophores, and therefore, such a result agrees with any interpretation. So we have no definitive experimental result to choose among the different cases, and the only way is through a comparison with the properties of **4**. Because of the similarities between the systems, we propose that even in **3** the energy-transfer process is hardly efficient; the predominance of MLCT<sub>2</sub> luminophore would also in this case largely be due to a difference in the absorption properties of the two chromophores, in particular to the better absorption properties of MLCT<sub>2</sub> over those of MLCT<sub>1</sub> (see Absorption Spectra), rather than to an effective energy-transfer process.

Our results suggest that photoinduced energy transfer across the ester-linked bridging ligands is barely efficient in the systems studied here, although it seems to occur to some extent. However, we would like to point out that this does not mean that ester-linked connectors are not appropriate for this type of study. In fact, relatively fast and efficient photoinduced electron transfer takes place in porphyrin–quinone systems assembled via ester-linked connectors.<sup>53,54</sup> The low driving forces for energy transfer in our systems (around  $-0.07$  eV in both **3** and **4**; the energy levels of MLCT<sub>1</sub>, MLCT<sub>2</sub>, and MLCT<sub>3</sub> are approximated to the luminescence maxima of **2**, **7**, and **6**, respectively; such values do not correspond to the real energy levels, but their energy gap, the relevant values for our calculation, should be valid) could be responsible for the observed behavior, in connection with the reorganization energy needed for energy transfer in organometallic systems, which is usually larger than in metal complexes containing only polypyridine ligands.<sup>55</sup> Unfavorable energetics (low driving force and high reorganization energy) coupled with the weak electronic interaction between the partners, as shown by electrochemical results, may justify the low efficiency of the inter-component energy transfer in the studied cases.

**Acknowledgment.** We thank the Italian Ministero dell'Università e della Ricerca Scientifica e Tecnologica (MURST), the Consiglio Nazionale delle Ricerche (CNR), and the European Community TMR Program (Research Network on Nanometer Size Metal Complexes) for financial support.

**Supporting Information Available:** Procedure for determining the number of the electrons involved in the redox processes and cyclic and differential pulse voltammograms. This material is available free of charge via the Internet at <http://pubs.acs.org>.

IC000212X

(52) Because of the different absorption and emission properties, the ratio of Ir-based and Re-based contributions to the emission output is more than 10 in dichloromethane, the solvent in which the possibility to resolve two lifetimes was higher because of the larger difference in the intrinsic lifetimes of the two subunits (Table 2). The situation was even worse in the other solvents, where the lifetimes are closer to one another.

(53) Cowan, J. A.; Sanders, J. K. M.; Beddard, G. S.; Harrison, R. J. *J. Chem. Soc., Chem. Commun.* **1987**, 55.

(54) Irvine, M. P.; Harrison, R. J.; Beddard, G. S.; Leighton, P.; Sanders, J. K. M. *Chem. Phys.* **1986**, *104*, 315.

(55) In the organometallic systems like the ones studied here, the MLCT states have partial LLCT character so that the dipole changes in the excited state compared to those in the ground state are more significant and a relatively large solvent reorganization energy is expected.